An Interpolated ab Initio Quantum Scattering Study of the Temperature Dependence of the $CH_3 + HBr \rightarrow CH_4 + Br$ Reaction†

Hua-Gen Yu‡ and Gunnar Nyman*

Department of Chemistry, Physical Chemistry, Göteborg University, S-412 96 Göteborg, Sweden

Received: September 27, 2000; In Final Form: December 6, 2000

An interpolated ab initio quantum scattering (AIQS) study for the $CH_3 + HBr \rightarrow CH_4 + Br$ reaction is presented. The ab initio calculation of energy points has been done using the UMP2/6-311G(3df,d,p) level of theory. Interpolation between the energy points was done using a recently developed generalized discrete variable representation (GDVR) approach. The quantum scattering calculations were performed using a reduced dimensionality rotating line umbrella (RLU) model. The UMP2 results give a vibrationally adiabatic ground-state barrier height of 0.69 kcal/mol for the forward reaction. An unstable van der Waals complex $CH_3\cdots HBr$ was also obtained. This complex plays only a minor role in the reaction dynamics. Calculated thermal rate coefficients show a strong nonlinear Arrhenius behavior. Below 550 K they have a negative temperature dependence, whereas a positive activation energy was obtained at higher temperatures. It was found that placing one quantum of energy in the vibrational mode of the H−Br bond stretch enhances the reactivity, whereas one quantum in the umbrella mode of CH_3 has the opposite effect. Finally, a comparison of calculated thermal rate coefficients with experimental results is made.

1. Introduction

Reactions of alkyl radicals (R) with hydrogen halides (HX, X = I, Br, and Cl) have been extensively studied during the past decades.[1−9] This is due to their importance for fundamental chemical kinetics and thermodynamics. The measured rate coefficients can be used to determine the heats of formation for the alkyl radicals. Early measurements showed that these radical reactions were activated processes characterized by small positive activation energies.[1−4,8] However, since 1988, negative activation energies with large rate coefficients have been observed using laser flash photolysis techniques for some small alkyl radical R + HX (X = I, Br, and Cl) reactions.[5−7,9] Although this finding can seem surprising for simple hydrogen transfer reactions, the heats of formation obtained for these alkyl radicals are in good agreement with those obtained from studies of bond dissociation and recombination rates. On the other hand, other recent direct kinetic studies using the very low-pressure reactor technique resulted in normal rate coefficients with positive activation energies for the *t*-C_4H_9 + DBr and C_2H_5 + HBr reactions.[8,10]

The measurements that lead to negative activation energies and large rate coefficients in the R + HX (X = I, Br, and Cl) reactions were recently assessed by Benson and Dobis.[8] They argued that highly vibrationally excited reactants might be involved in the experiments, resulting in a negative activation energy. To clarify this issue, Krasnoperov and Mehta[9] reinvestigated the CH_3 + HBr and CH_3 + Br reactions over an extended buffer gas density range using the laser photolysis technique, where the pressure used is high enough to completely quench any vibrationally excited species on the time scale of the experiments. They ruled out errors due to contributions from vibrationally excited species but do not draw definite conclusions about the activation energy.

The $CH_3 + HBr \rightarrow CH_4 + Br$ reaction was studied by Chen et al.[11,12] using RRKM theory applied to a potential energy surface defined by G1 ab initio calculations. The G1 results give a saddle point with a collinear "Br−H−CH_3" structure in C_{3v} geometry and a van der Waals complex $CH_3\cdots HBr$ with a small binding energy of 0.28 kcal/mol (including the zero point energies). A statistical decay from the van der Waals complex to products or back to reactants was assumed. The vibrationally adiabatic ground-state barrier height (V_a^G) obtained was 0.67 kcal/mol for the forward process. However, in the RRKM calculations, the authors had to adjust the V_a^G to be −0.11 kcal/mol to fit the experimental rate coefficients, implying a negative activation energy.

The assumption of statistical behavior and the Wigner tunneling correction used in the theoretical study might be questioned because the van der Waals well is so shallow and the V_a^G value is negative. In addition, the most recent rate coefficients[6,7,9] are a factor of 2 higher than those used by Chen et al.[12] We thus find it motivated to theoretically investigate the $CH_3 + HBr \rightarrow CH_4 + Br$ reaction again.

In the present work, a reduced dimensionality quantum scattering approach[13−15] has been used to study the $CH_3 + HBr \rightarrow CH_4 + Br$ reaction. The potential energy surface employed was directly interpolated from a set of ab initio energy points using a generalized discrete variable representation (GDVR) method.[16] The main goal is to investigate the effects on the thermal rate coefficients of tunneling, recrossing, vibrationally excited reagents, and the vibrationally adiabatic ground-state barrier height. The temperature dependence of the thermal rate coefficient and the validity of an RRKM approach to this reaction is discussed.

* E-mail: nyman@phc.gu.se.

† Part of the special issue "Aron Kuppermann Festschrift".

‡ Present address: Department of Chemistry, Brookhaven National Laboratory, Upton, NY 11973-5000.

10.1021/jp0035075 CCC: $20.00
Published on Web 02/10/2001

2. Quantum Dynamics

In the quantum scattering calculations a three-dimensional rotating line umbrella (RLU) model[13−15,17] was used. For the $CH_3 + HBr \rightarrow CH_4 + Br$ reaction, the RLU model treats the umbrella vibrational mode of CH_3/CH_4 and the H−Br and H−CH_3 reactive bond stretches explicitly, while the remaining vibrational degrees of freedom are taken into account statistically. In the RLU model the system is kept in C_{3v} symmetry throughout the reaction.

The RLU Hamiltonian of the system is written in the hypercylindrical coordinates (ρ, φ, z) as

$$\hat{H}(\rho, \varphi, z) = -\frac{\hbar^2}{2\mu}\left[\frac{1}{\rho^3}\frac{\partial}{\partial\rho}\rho^3\frac{\partial}{\partial\rho} + \frac{1}{\rho^2}\frac{\partial^2}{\partial\varphi^2}\right] - \frac{\hbar^2}{2}\frac{\partial}{\partial z}G(z)\frac{\partial}{\partial z} + \frac{\hat{J}^2}{2I(z)} + V_{\text{eff}}(\rho, \varphi, z) \quad (1)$$

with the volume element

$$d\tau = \rho^3 d\rho d\varphi dz \sin\theta d\theta d\phi$$

where

$$I(z) = \mu\rho^2 + \mu_z z^2$$

$$\mu = \left[\frac{m_{\text{Br}} m_{\text{H}}(m_{\text{C}} + 3m_{\text{H}})}{m_{\text{T}}}\right]^{1/2}$$

$$\mu_z = \frac{3m_{\text{C}}m_{\text{H}}}{m_{\text{C}} + 3m_{\text{H}}}$$

$$m_{\text{T}} = m_{\text{Br}} + m_{\text{H}} + m_{\text{C}} + 3m_{\text{H}}$$

$$G(z) = \frac{R_3^2 - z^2}{\mu_z(R_3^2 + 3m_{\text{H}}z^2/m_{\text{C}})}$$

and the total angular momentum operator is

$$\hat{J}^2 = -\hbar^2\left[\frac{1}{\sin\theta}\frac{\partial}{\partial\theta}\sin\theta\frac{\partial}{\partial\theta} + \frac{1}{\sin^2\theta}\frac{\partial^2}{\partial\phi^2}\right] \quad (2)$$

Here m_{Br}, m_{C}, and m_{H} are the masses of the Br, C, and H atoms, respectively. The terms θ and ϕ are the spherical angles describing the spatial orientation of the linear Br−H−C axis in the CH_4Br molecule. In eq 1, $V_{\text{eff}}(\rho, \varphi, z)$ is an effective potential energy surface, see section 3.

The time independent Schrödinger equation of the system was solved using the log-derivative algorithm of Manolopoulos[18,19] in a partial wave expansion basis set. The resulting coupled channel equations were propagated from a small hyperradius ρ to a large ρ. The adiabatic basis set was calculated using the guided spectral transform (GST) algorithm due to the authors.[17,20−25] In the asymptotic region, where ρ is large, the S-matrix was extracted using the hyperspherical projection method.[13,14,20] It gives the scattering S-matrix as

$$S^J(E) = -\mathbf{k}^{1/2}\mathbf{W}^{-1}\mathbf{W}^*\mathbf{k}^{-1/2} \quad (3)$$

with

$$\mathbf{W} = [\mathbf{Y}(\rho_i)X^{(1)} - X^{(3)}] + i[\mathbf{Y}(\rho_i)X^{(2)} - X^{(4)}] \quad (4)$$

where $\mathbf{k}$ is a diagonal matrix with the elements $(\mathbf{k})_{n'n} = k_n\delta_{n'n}$, and where k_n is a wave vector. $\mathbf{Y}$ is the log-derivative matrix. The projection matrices $\mathbf{X}^{(i)}$ have been given in refs 13 and 14.

From the S-matrix, the state-to-state reaction probability for the reaction $CH_3(v_2) + HBr(v) \rightarrow CH_4(v_{3b}, v_4) + Br$ is defined by

$$P^J_{vv_2\rightarrow v_{3b}v_4} = |S^J_{vv_2\rightarrow v_{3b}v_4}|^2 \quad (5)$$

where the vibrational quantum numbers v, v_{3b}, v_2, and v_4 refer to the H−Br stretch, the reactive H−CH_3 stretch and the umbrella modes in CH_3 and CH_4, respectively. The cumulative reaction probability (CRP), $N(E, J)$, can be calculated by summing the state-to-state reaction probabilities over all final and initial states, i.e.

$$N(E, J) = \sum_{vv_2}\sum_{v_{3b}v_4} P^J_{vv_2\rightarrow v_{3b}v_4} \quad (6)$$

The thermal rate coefficient is calculated from ref 25

$$k(T) = \sum_J (2J+1)k_{\text{J}}(T) \quad (7)$$

$$k_{\text{J}}(T) = \frac{Q(T)Q^{\ddagger}_{\text{J}}(T)}{2\pi\hbar Q_r(T)}\int_{-\infty}^{+\infty} dE \exp\{-E/kT\}N(E, J) \quad (8)$$

where

$$Q^{\ddagger}_{\text{J}}(T) = \sum_{K=-J}^{J} \text{e}^{-E_K/kT} \quad (9)$$

and

$$E_K = (A^{\ddagger} - B^{\ddagger})K^2 \quad (10)$$

$Q(T)$ is the partition function at the transition state for all vibrational modes not explicitly treated in the RLU scattering calculations. $A^{\ddagger}$ and $B^{\ddagger}$ are the rotational constants of the transition state $CH_3\cdots H\cdots Br$ treated as a symmetric top. $Q_r(T)$ is the reactant partition function per unit volume. To obtain eq 8, the K-shifting approximation[26−28] has been invoked.

Vibrationally state-selected rate coefficients $k_{vv_2}(T)$ for the reaction $CH_3(v_2) + HBr(v) \rightarrow CH_4 + Br$ are calculated from

$$k_{vv_2}(T) = \sum_J (2J+1)k^J_{vv_2}(T) \quad (11)$$

$$k^J_{vv_2}(T) = \frac{Q(T)Q^{\ddagger}_{\text{J}}(T)}{2\pi\hbar Q'}{}_r(T)\int_{-\infty}^{+\infty} dE \exp\{-E/kT\}N_{vv_2}(E - \epsilon_{vv_2}, J) \quad (12)$$

with the initial state-selected cumulative reaction probabilities

$$N_{vv_2}(E, J) = \sum_{v_{3b}v_4} P^J_{vv_2\rightarrow v_{3b}v_4} \quad (13)$$

where $Q'_r(T)$ is the reactant partition function per unit volume but excluding the contributions from the two vibrational modes (v, v_2) of HBr and CH_3. ϵ_{vv_2} is the vibrational energy referenced to the ($v = 0$, $v_2 = 0$) level.

The ground-state tunneling coefficient, η^G, and ground-state transmission coefficient, κ^G, are defined as[25]

$$\eta^G = \frac{k_{00}(T)}{k_{00}^*(T)} = \frac{\sum_J (2J+1) Q_J^{\ddagger}(T) \int_{-\infty}^{\infty} dE \exp(-E/kT) N_{00}(E, J)}{\sum_J (2J+1) Q_J^{\ddagger}(T) \int_{E_J^*}^{\infty} dE \exp(-E/kT) N_{00}(E, J)} \quad (14)$$

$$\kappa^G = \frac{k_{00}(\mathrm{T})}{k_{00}^{\mathrm{TST}}(T)} = \frac{\sum_J (2J+1) Q_J^{\ddagger}(T) \int_{-\infty}^{\infty} dE \exp(\text{-}E/kT) N_{00}(E, J)}{kT \sum_J (2J+1) Q_J^{\ddagger}(T) \exp(-E_J^*/kT)} \quad (15)$$

where $E_J^* = V_a^G + J(J+1)B^{\ddagger}$ is an effective vibrational ground-state barrier height for a total angular momentum J. The term $k_{00}^*(T)$ is a rate coefficient for reaction out of the ground state of the reactants, which excludes tunneling. It is obtained by setting the lower limit in eq 12 to E_J^*, multiplying by $2J + 1$ and summing over J. The term $k_{00}^{TST}(T)$ is the conventional transition state theory (TST) rate coefficient for reaction out of the ($v = 0$, $v_2 = 0$) state.

The frequencies and geometries at the stationary points that were used to evaluate the partition functions in eqs 8 and 12 are given in Table 1.

3. Potential Energy Surface

Ab initio electronic structure calculations were performed with the GAUSSIAN 98 code.[29] The full second-order Møller−Plesset (UMP2) perturbation theory has been used with a 6-311G(3df,d,p) basis set.[30,31] This basis set consists of a triple split 6-311G basis set[31] with polarization functions having exponential parameters $\alpha_p = 0.75$ for the hydrogens, $\alpha_d = 0.626$ for the carbon atom, and $\alpha_d = 1.353$, 0.451, 0.15033 and $\alpha_f = 0.560$ for the bromine atom.

Calculated structures and frequencies of the stationary points for the $CH_3 + HBr \rightarrow CH_4 + Br$ reaction are given in Table 1. There is a van der Waals complex with C_{3v} symmetry in the entrance channel. It has an energy of −3.34 kcal/mol relative to the $CH_3 + HBr$ limit. However, with the zero point energies added, this complex is unstable. In contrast, the G1 theory[11] predicted it to be 0.28 kcal/mol below the $CH_3 + HBr$ limit. Also obtained is a C_{3v} symmetric transition state with a long H−CH_3 bond. The transition state is lower in energy (2.16 kcal/mol) than the reactants. If the harmonic zero point energies are taken into account, we obtain a vibrationally adiabatic ground-state barrier height V_a^G symmetric transition state with a long H−CH3 bond. The transition state is low, $G1 = 0.69$ kcal/mol, which is consistent with the G1 result 0.67 kcal/mol.[11] These stationary point comparisons suggests that the UMP2/6-311G-(3df,d,p) method may describe the reaction quite well.

In the RLU quantum scattering calculations, the three-dimensional potential energy surface was interpolated from 1296 energy points using the GDVR method.[16,25] The energy points were precomputed using the UMP2/6-311G(3df,d,p) theory for C_{3V} geometries for the CH_3HBr molecule with the C−H bond length of the CH_3 moiety held fixed at 2.0464 a_0, i.e, the value at the transition state. Twelve points were used for each of the H−Br ($R_{HBr} = 1.55 \sim 8.0\ a_0$) and H−$CH_3$ ($R_{CH} = 1.35 \sim 7.0\ a_0$) bond stretches, while 9 points were used for the umbrella coordinate $z = -1.65 \sim 1.65\ a_0$.

In the interpolation procedure, the logarithm $x_i = \ln R_i$ was employed for both the R_{HBr} and R_{CH} variables. Furthermore, for the reactant channel, the long-range interaction potential was extrapolated assuming a dipole−quadrupole $C_4(R_{HBr}, z)/R_{CH}^{-4}$ behavior. $C_4(R_{HBr}, z)$ was determined by interpolation between the ab initio energies for the two largest R_{CH} distances for each R_{HBr} and z value on the grid. The potential energy surface, $V(R_{HBr}, R_{CH}, z)$, is illustrated in Figure 1 with the umbrella coordinate z optimized. Both the van der Waals complex and the transition state are clearly seen.

TABLE 1: Calculated Geometric Structures, Energies, and Harmonic normal Mode Frequencies of Stationary Points for the $CH_3 + HBr \rightarrow CH_4 + Br$ Reaction at the UMP2/6-311G(3df,d,p) Level of Theory (length in Bohr; angles in degrees)

species	parameter	value	energy/au	mode	freq/cm^{-1a}
Br			−2572.93106		
HBr	R_{HBr}	2.6758	−2573.57183	σ	2592
$CH_3(D_{3h})$	R_{CH}	2.0415	−39.72506	a_2''	417
				e′	1376
				a_1'	3008
				e′	3216
$CH_4(T_d)$	R_{CH}	2.0617	−40.39804	t_1	1298
				e	1501
				a_1	2918
				t_2	3048
$CH_3'\cdots HBr$	R_{HBr}	2.6933	−2613.30221	$\nu_1(a_1)$	3005
(complex, C_{3V})	R_{CH}	4.3521		ν_2	2479
	$R_{CH'}$	2.0411		ν_3	745
	$\angle HCH'$	93.46		ν_4	29
				ν_5(e)	3211
				ν_6	1380
				ν_7	619
				ν_8	410
$CH_3'\cdots HBr$	R_{HBr}	2.8312	−2613.30032	$\nu_1(a_1)$	2980
(TS, C_{3V})	R_{CH}	3.0486		ν_2	1488
	$R_{CH'}$	2.0464		ν_3	892
	$\angle HCH'$	98.48		ν_4	297*i*
				$\nu_5(e)$	3184
				ν_6	1386
				ν_7	804
				ν_8	543

[a] The UMP2/6-311G(3df,d,p) frequencies are scaled by 0.95.[32]

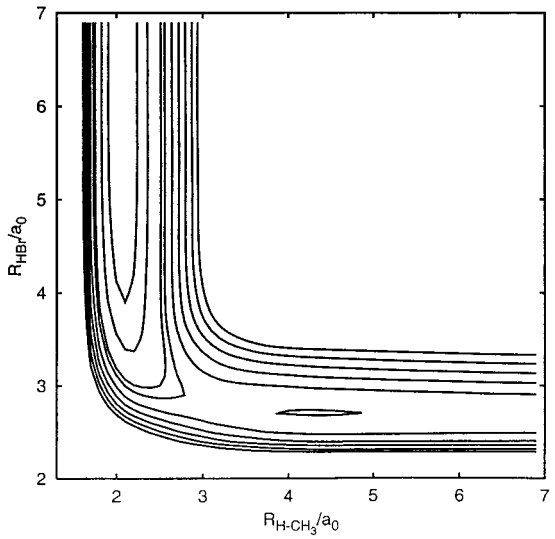

Figure 1. The potential energy surface for the $CH_3 + HBr \rightarrow CH_4 + Br$ reaction in C_{3v} symmetry, with the umbrella coordinate optimized. The contours start at 0.09 eV with an interval of 0.20 eV. Energies are relative to the $CH_4 + Br$ limit.

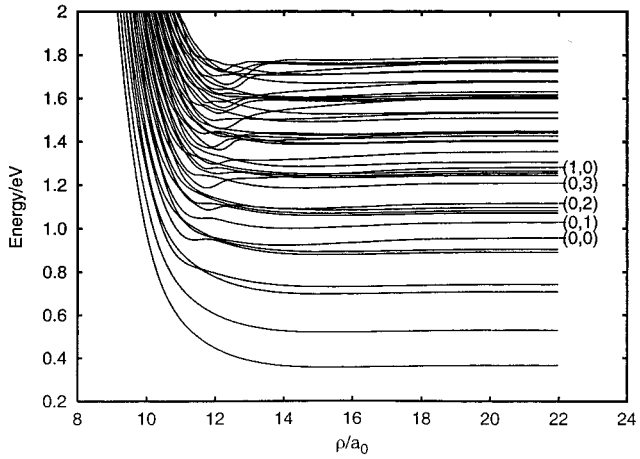

Figure 2. Hyperspherical adiabats for the $CH_3 + HBr \rightarrow CH_4 + Br$ reaction as a function of hyperradius for the total angular momentum $J = 0$. (v, v_2) refer to $HBr(v) + CH_3(v_2)$.

The effective potential energy surface used in the dynamics calculations was obtained by

$$V_{\text{eff}}(R_{\text{HBr}}, R_{\text{CH}}, z) = V(R_{\text{HBr}}, R_{\text{CH}}, z) + \Delta V_{\text{corr}} \qquad (16)$$

with

$$\Delta V_{\text{corr}} = V_c[1 - \tanh\gamma(R_{\text{CH}} - R^{\text{e}}_{\text{CH}})] \qquad (17)$$

where the parameters are $\gamma = 0.2522a_0^{-1}$, $R^{\text{e}}_{\text{CH}} = 0.7583a_0$, and $V_c = 0.198$ eV. This correction is mainly made for the H−CH_3 bending normal modes of CH_4 so that a vibrationally adiabatic ground-state barrier height of 0.69 kcal/mol is produced in the reduced dimensionality quantum scattering calculations.

4. Results and Discussion

In the scattering calculations, the coupling matrix was expressed in a direct product DVR basis. We have used 70 sine-DVRs for n and 35 Fourier DVRs for z, spanning the range $[-1.65, 1.65]a_0$. The final DVR basis was truncated by a potential energy threshold of 3.5 eV in each sector. A set of 60 coupled channel equations were propagated using 278 sectors from hyperradius $\rho = 8.0\ a_0$ to $\rho = 22.0\ a_0$, where the scattering S-matrix elements were extracted.

Figure 2 shows the adiabatic energy levels as a function of the hyperradius. As this hydrogen abstraction process is a heavy−light−heavy (HLH) reaction, these adiabats reflect many dynamical features. For instance, the low-lying adiabats are repulsive while there are wells on some of the adiabats with higher energy. The wells give rise to resonances which can be seen in Figure 3 as structure in the reaction probabilities. At low kinetic energies, there are just two broad resonances, suggesting that the shallow van der Waals complex does not play an important role in the dynamics.

Calculated rate coefficients, ground-state tunneling and transmission coefficients are given in Table 2. The thermal rate coefficients show a strong nonlinear Arrhenius behavior. Up to 550 K, a negative temperature dependence was obtained, even though the vibrationally adiabatic ground-state barrier height is positive ($V_a^G = 0.69$ kcal/mol). This largely results from the quantum tunneling effects associated with this light atom transfer reaction. We note that the Wigner tunneling coefficients used in the RRKM calculations[12] are lower than the ones obtained from the RLU calculations. However, for this HLH reaction, the recrossing factor ($\eta^G/\kappa^G \sim 3$) is large, which partially compensates for the different tunneling coefficients. Above 550 K, the calculated thermal rate coefficients give a positive activation energy. The temperature dependence is, however, rather small as the rate coefficient only increases by about 50% on raising the temperature from 550 to 1100 K.

It is interesting to study the effect of reactant vibrational excitation on the reactivity. As shown in Figure 4, placing one quantum of energy in the CH_3 umbrella mode makes the reaction slower. The corresponding rate coefficient, $k_{01}(T)$, has a positive

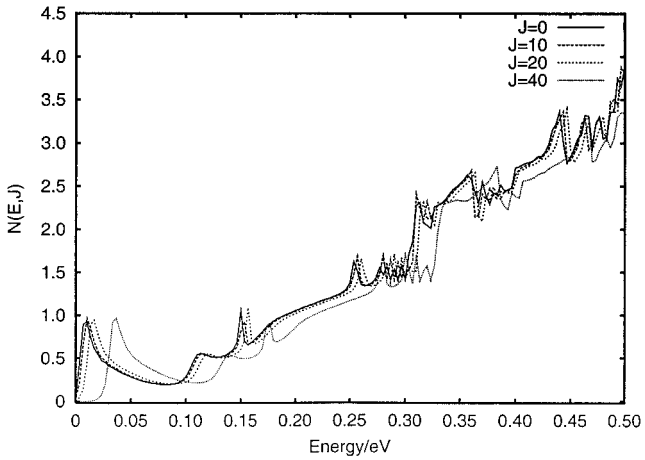

Figure 3. Calculated cumulative reaction probabilities $N(E, J)$ vs energy for the $CH_3 + HBr \rightarrow CH_4 + Br$ reaction for several total angular momenta J.

TABLE 2: Calculated Thermal Rate Coefficients ($k(T)/10^{-12}$ cm^3 molecule^{-1} s^{-1}), Initial State-Selected Rate Coefficients ($k_{v v_2}(T)/10^{-12}$ cm^3 molecules^{-1} s^{-1}), Ground State Tunneling (η^G), and Transmission (κ^G) Coefficients for the $CH_3 + HBr \rightarrow CH_4 + Br$ Reaction

T/K	$k(T)$	$k_{00}(T)$	$k_{01}(T)$	$k_{10}(T)$	η^G	$W(297i)^a$	κ^G	$k(T)^b$	η^{Gb}
150	1.62	1.62	0.089	3.27	17.0	1.34	6.1	2.87	3.2
200	1.20	1.21	0.13	2.29	10.1	1.19	3.5	2.00	3.1
250	0.99	1.02	0.17	1.82	7.4	1.12	2.6	1.64	3.1
300	0.88	0.93	0.20	1.57	6.0	1.08	2.0	1.46	3.1
350	0.81	0.88	0.25	1.42	5.1	1.06	1.7	1.36	3.1
400	0.78	0.86	0.28	1.34	4.5	1.05	1.5	1.30	3.1
500	0.76	0.86	0.36	1.29	3.7	1.03	1.3	1.28	2.9
600	0.77	0.91	0.44	1.31	3.2	1.02	1.1	1.30	2.7
800	0.88	1.08	0.63	1.46	2.5	1.01	0.9	1.44	2.4
1000	1.06	1.33	0.87	1.70	2.2	1.01	0.8	1.65	2.1

[a] Wigner tunneling correction $[1-(h\nu/k_BT)^2/24]$ using an imaginary frequency of $297i$ cm^{-1}. [b] These values were obtained with a $V_a^G = 0.0$ kcal/mol potential energy surface.

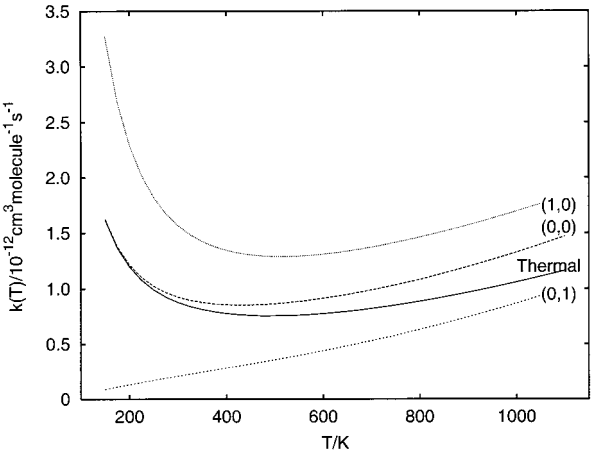

Figure 4. Calculated thermal rate coefficients and initial state-selected rate coefficients, denoted by (v, v_2) for the $HBr(v) + CH_3(v_2)$ reaction.

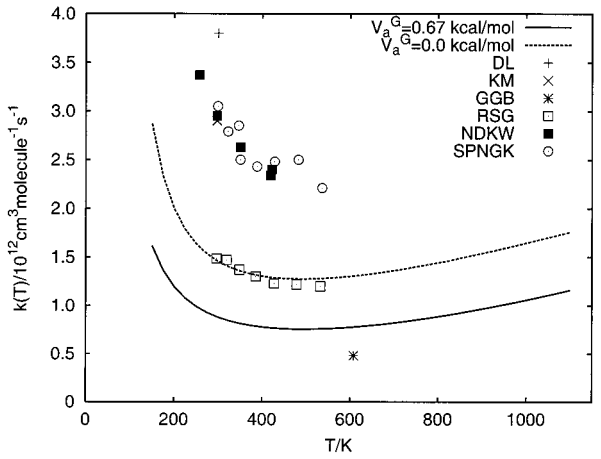

Figure 5. Comparison of calculated thermal rate coefficients with experimental results for the CH_3 + HBr reaction. The acronyms in the figure refer to experimental results as follows: DL,[4] KM,[9] GGB,[3] RSG,[5] NDKW,[6] SPNGK.[7]

temperature dependence. An explanation for this is that the reaction approximately behaves vibrationally adiabatic and, because the umbrella mode frequency increases as the reaction proceeds, exciting this mode increases the vibrationally adiabatic barrier height, thereby decreasing the reaction rate.

If we put one quantum of energy in the H−Br stretch motion, the rate coefficients roughly increase a factor of 2 compared to the ground-state results, with a temperature dependence that is similar to that of the thermal rate coefficients. We have also noticed that the translational energy is more efficient in enhancing the reaction than the vibrational energies are. This observation is consistent with the shape of the potential energy surface, see Figure 1, which shows an early transition state.

The calculated rate coefficients are slightly larger than the experimental value 0.48×10^{-12}cm^3 molecule^{-1} s^{-1}, obtained as a low estimate of the average value in the range 608 K−1000 K.[3−5] Figure 5 shows a comparison of calculated thermal rate coefficients with several experimental results.[4−7,9] The present results are roughly a factor of 3 smaller than some of these measurements.[4,6,7,9]

To investigate the effect of the barrier height of the potential energy surface, we have used a surface with a $V_a^G = 0.00$ kcal/mol, obtained by setting $V_c = 0.150$ eV in eq 17. The resulting rate coefficients are given in Table 2 and also shown in Figure 5. They are about 70% larger than in the $V_a^G = 0.69$ kcal/mol case, but with similar temperature dependence. If the V_a^G is further reduced, to be negative, the rates do not change significantly. A further increase in the rates could have been expected as for $J > 0$, a negative V_a^G would remove or decrease the centrifugal barrier. Either this has only a small effect on the rate coefficients or tunneling through the centrifugal barrier is important enough to make the net effect small. It is seen in Figure 5 that the $V_a^G = 0.00$ kcal/mol results are in very good agreement with the experimental values by Russell et al.[5] Their values are, however, now believed to have been incorrectly obtained[6,7] and more recently measured rate coefficients are a factor of 2 larger.[7]

5. Conclusions

We have performed an interpolated ab initio quantum scattering (AIQS) study for the CH_3 + HBr → CH_4 + Br reaction using the rotating line umbrella (RLU) model. The potential energy surface was interpolated from 1296 UMP2/6-311G(3df,d,p) energy points. The UMP2 theory predicts a transition state with C_{3v} symmetry and a vibrationally adiabatic ground-state barrier height of 0.69 kcal/mol. There is a van der Waals complex, CH_3···HBr, in the entrance channel, which however is unstable.

The calculated thermal rate coefficients show a strong nonlinear Arrhenius behavior. At lower temperatures, the rate coefficients have a negative temperature dependence, while a positive activation energy was obtained at higher temperatures. The negative temperature dependence is largely due to tunneling effects. Further, it was found that the shallow van der Waals complex has only minor effects on the dynamics, which suggests that the statistical decay assumption made in the previous RRKM study on this reaction may not be valid, even if good agreement with experimental results may be found.

Vibrational excitation of the reactants has also been investigated. Exciting the vibrational mode of the H−Br bond stretch can enhance the reaction, whereas exciting the umbrella mode of CH_3 has the opposite effect. This is consistent with the latter case, giving a positive activation energy over the whole temperature range 150−1100 K. In contrast, the temperature dependence for the $CH_3(v_2 = 0)$ + HBr($v = 1$) reaction is similar to that of the calculated thermal rate coefficients.

Finally, the results show that the thermal rate coefficients we have calculated using the RLU model and our AIQS approach are in good agreement with the experimental results by Gac et al.[3,5] They are, however, a factor of 3 smaller than most of the more recent experimental results. Although the calculated rate coefficients can be increased by using a potential energy surface with a smaller V_a^G value, it is still hard to fit the largest experimental rate coefficients measured.

Acknowledgment. H.G.Y. thanks Profs. Sidney W. Benson and Lev N. Krasnoperov for fruitful discussions. The calculations were carried out on a Silicon Graphics Power Challenge supercomputer at Chalmers University of Technology and Göteborg University. This research has been supported by the Swedish Natural Science Research Council (NFR).

References and Notes

(1) Williams, R. R., Jr.; Ogg, R. A., Jr. *J. Chem. Phys*. **1947**, *15*, 696.
(2) Farren, J.; Gilbert, J. R.; Linnett, J. W.; Reid, I. A. *Transactions of the Faraday Society* **1964**, *60*, 740.
(3) Gac, N. A.; Golden, D. M.; Benson, S. W. *J. Am. Chem. Soc*. **1969**, *91*, 3091.
(4) Donaldson, D. J.; Leone, S. R. *J. Phys. Chem*. **1986**, *90*, 936.
(5) Russell, J. J.; Seetula, J. A.; Gutman, D. *J. Am. Chem. Soc*. **1988**, *110*, 3092.
(6) Nicovich, J. M.; van Dijk, C. A.; Kreutter, K. D.; Wine, P. H. *J. Phys. Chem*. **1991**, *95*, 9890.
(7) Seakins, P. W.; Pilling, M. J.; Niiranen, J. T.; Gutman, D.; Krasnoperov, L. N. *J. Phys. Chem*. **1992**, *96*, 9847.
(8) Benson, S. W.; Dobis, O. *J. Phys. Chem. A* **1998**, *102*, 5175.
(9) Krasnoperov, L. N.; Mehta, K. *J. Phys. Chem. A* **1999**, *103*, 8008.
(10) Dobis, O.; Benson, S. W. *J. Am. Chem. Soc*. **1995**, *117*, 8171.
(11) Chen, Y.; Tschuikow-Roux, E.; Rauk, A. *J. Phys. Chem*. **1991**, *95*, 9832.
(12) Chen, Y.; Rauk, A.; Tschuikow-Roux, E. *J. Phys. Chem*. **1991**, *95*, 9900.
(13) Yu, H. G.; Nyman, G. *Phys. Chem. Chem. Phys*. **1999**, *1*, 1181.
(14) Yu, H. G.; Nyman, G. *J. Chem. Phys*. **1999**, *111*, 6693.
(15) Yu, H. G.; Nyman, G. *Chem. Phys. Lett*. **1999**, *312*, 585.
(16) Yu, H. G.; Andersson, S.; Nyman, G. *Chem. Phys. Lett*. **2000**, *321*, 275.
(17) Yu, H. G.; Nyman, G. *Chem. Phys. Lett*. **1998**, *298*, 27.
(18) Manolopoulos, D. E. *J. Chem. Phys*. **1986**, *85*, 6425.
(19) Manolopoulos, D. E.; D'Mello, M.; Wyatt, R. E. *J. Chem. Phys*. **1989**, *91*, 6096.
(20) Yu, H. G.; Nyman, G. *J. Chem. Phys*. **1999**, *110*, 7233.
(21) Yu, H. G.; Nyman, G. *J. Chem. Phys*. **1999**, *110*, 11133.
(22) Yu, H. G.; Nyman, G. *J. Chem. Phys*. **2000**, *112*, 238.
(23) Yu, H. G.; Nyman, G. *J. Chem. Phys*. **1999**, *111*, 3508.

(24) Yu, H. G.; Nyman, G. *J. Chem. Phys.* **2000**, *112*, 3935.
(25) Yu, H. G.; Nyman, G. *J. Chem. Phys.* **2000**, *113*, 8936.
(26) Nyman, G.; Clary, D. C. *J. Chem. Phys.* **1994**, *101*, 5756.
(27) Manthe, U.; Seideman, T.; Miller, W. H. *J. Chem. Phys.* **1993**, *99*, 10078.
(28) Bowman, J. M. *Adv. Chem. Phys.* **1985**, *61*, 116.
(29) Frisch, M. J.; Trucks, G. W.; Schlegel, H. B.; Scuseria, G. E.; Robb, M. A.; Cheeseman, J. R.; Zakrzewski, V. G.; Montgomery, J. A., Jr.; Stratmann, R. E.; Burant, J. C.; Dapprich, S.; Millam, J. M.; Daniels, A. D.; Kudin, K. N.; Strain, M. C.; Farkas, O.; Tomasi, J.; Barone, V.; Cossi, M.; Cammi, R.; Mennucci, B.; Pomelli, C.; Adamo, C.; Clifford, S.; Ochterski, J.; Petersson, G. A.; Ayala, P. Y.; Cui, Q.; Morokuma, K.; Malick, D. K.; Rabuck, A. D.; Raghavachari, K.; Foresman, J. B.; Cioslowski, J.; Ortiz, J. V.; Stefanov, B. B.; Liu, G.; Liashenko, A.; Piskorz, P.; Komaromi, I.; Gomperts, R.; Martin, R. L.; Fox, D. J.; Keith, T.; Al-Laham, M. A.; Peng, C. Y.; Nanayakkara, A.; Gonzalez, C.; Challacombe, M.; Gill, P. M. W.; Johnson, B. G.; Chen, W.; Wong, M. W.; Andres, J. L.; Head-Gordon, M.; Replogle, E. S.; Pople, J. A. *Gaussian 98*, revision A.3; Gaussian, Inc.: Pittsburgh, PA, 1998.
(30) McLean, A. D.; Chandler, G. S. *J. Chem. Phys.* **1980**, *72*, 5639.
(31) Krishnan, R.; Binkley, J. S.; Seeger, R.; Pople, J. A. *J. Chem. Phys.* **1980**, *72*, 650.
(32) Hehre, W. J.; Radom, L.; Schleyer, P. v. R.; Pople, J. A. *Ab Initio Molecular Orbital Theory*; Wiley, New York, 1989.